Characterizing inertial and convective optical turbulence by detrended fluctuation analysis.

Gustavo Funes[a], Eduardo Figueroa[b], Damián Gulich[a], Luciano Zunino[a,c] and Darío G. Pérez[b]

[a]Centro de Investigaciones Ópticas (CIOp), C.C. 3, 1897 Gonnet, Argentina.
[b] Instituto de Física, Pontificia Universidad Católica de Valparaíso (PUCV), 23-40025 Valparaíso, Chile.
[c]Departamento de Ciencias Básicas, Facultad de Ingeniería, Universidad Nacional de La Plata (UNLP), 1900 La Plata, Argentina.

ABSTRACT

Atmospheric turbulence is usually simulated at the laboratory by generating convective free flows with hot surfaces, or heaters. It is tacitly assumed that propagation experiments in this environment are comparable to those usually found outdoors. Nevertheless, it is unclear under which conditions the analogy between convective and isotropic turbulence is valid; that is, obeying Kolmogorov isotropic models. For instance, near-ground-level turbulence often is driven by shear ratchets deviating from established inertial models. In this case, a value for the structure constant can be obtained but it would be unable to distinguish between both classes of turbulence. We have performed a conceptually simple experiment of laser beam propagation through two types of artificial turbulence: isotropic turbulence generated by a turbulator [Proc. SPIE **8535**, 853508 (2012)], and convective turbulence by controlling the temperature of electric heaters. In both cases, a thin laser beam propagates across the turbulent path, and its wandering is registered by a position sensor detector. The strength of the optical turbulence, in terms of the structure constant, is obtained from the wandering variance. It is expressed as a function of the temperature difference between cold and hot sources in each setup. We compare the time series behaviour for each turbulence with increasing turbulence strength by estimating the Hurst exponent, H, through *detrended fluctuation analysis* (DFA). Refractive index fluctuations are inherently fractal; this characteristic is reflected in their spectra power-law dependence—in the inertial range. This fractal behaviour is inherited by time series of optical quantities, such as the wandering, by the occurrence of long-range correlations. By analyzing the wandering time series with this technique, we are able to correlate the turbulence strength to the value of the Hurt exponent. Ultimately, we characterize both types of turbulence.

Keywords: multifractal detrended fluctuation analysis, Hurst exponent, beam wandering, angle-of-arrival, non-Kolmogorov turbulence

1. INTRODUCTION

Deviations from the well-known Obukov-Kolmogorov (OK) theory on passive scalars are quite accepted nowadays. The pioneer work of Vilar & Haddon has opened the door to the existence of a generalized turbulence spectra.[1] They were the first to propose a model for the refractive index fluctuations spectrum where the power exponent can differ from the usual 11/3. They argue, that even though many experimental results have shown reasonable agreement with the OK model, some scintillations experiments found strong departures from it. Particularly, theoretical studies on scintillation variance have shown a strong dependence on the power exponent and the outer scale, thus making any determination of the structure constant highly questionable. Many contributions, theoretical and experimental, have dealt with non-Kolmogorov (NOK) models, to name a few: Stribling[2] studied the log-amplitude and phase variances in non-Kolmogorov turbulence; Beland[3] developed similar calculations, and established bounds for power exponent on the range $[3, 4)$; Dayton *et al.*,[4] and later Nicholls *et al.*,[5] has found experimental evidence, with a Shack-Hartmann sensor, of non-Kolmogorov behaviour on the phase structure

Further author information: (Send correspondence to D.G.P.)
D.G.P.: E-mail: dario.perez@ucv.cl
G.F.: E-mail: gfunes@ciop.unlp.edu.ar

Remote Sensing of Clouds and the Atmosphere XVIII; and Optics in Atmospheric Propagation and Adaptive Systems XVI, edited by Adolfo Comeron, et. al., Proc. of SPIE Vol. 8890, 889016
 · doi: 10.1117/12.2028698

function; finally, Gurvich & Belen'kĭ[6] introduced a model for stratospheric turbulence power spectrum, where non-Kolmogorov behaviour is more common. Most of the interest today in NOK turbulence resides is in modelling optical communication channels,[7–12] as near-to-the-ground turbulence tends to deviate the most.

Indeed, surface-layer turbulence is highly likely to be anisotropic (wind ratchets and uneven terrains are usually the source). Some have stated[7,8] that it could be a cause for deviations from the 11/3 exponent. Therefore, anisotropy and non-Kolmogorov behaviour may be linked. Recent works[13] have proposed a particular model for anisotropic non-Kolmogorov turbulence. Under it, the anisotropy arises as a multiplicative correction term also depending on the non-Kolmogorov power exponent.

Under the assumption that the refractive index perturbations due to the turbulence are Gaussian, we have proved[14] that Lévy fractional Brownian fields (LfBf) are a good model for the phase perturbations due to non-Kolmogorov turbulence, if the inner- and outer-scales are not accounted for. This very same model can be applied to the index itself; therefore, using the classical definition given to wave-front phase, in weak regime, it can be shown that index perturbations from a partially developed turbulence with Hurst exponent H produce phase fluctuations with exponent equal to $H + \frac{1}{2}$—5/6 for the Kolmogorov case. This is the expected exponent controlling the time-series obtained in each coordinate axis as we discussed in Ref. [15]. These Gaussian processes have a Hurst exponent in the range $(0.5, 1)$, representing a correlated signal. This is related to spectra with exponents from 3 to 4, which was validated in several works.[3,8,9]

Scale invariance and self-similarity for time series can be associated with a single type of structure characterized by a single exponent, H, or by composition of several sub-structures with certain local exponent, h. The former is called mono-fractal and the latter multi-fractal. The statistical characteristics (correlations for instance) of these series are dominated by these local exponents, being the first a special case of the latter. In recent years, a widely adopted method used for the determination of the fractal scaling properties and detection of long-range correlations in noisy and non-stationary time series is the *multifractal detrended fluctuation analysis* (MF-DFA). It is a highly robust and easy to implement technique, a detailed description of which can be found elsewhere.[16] The local exponent is a continuous function of the order q which is associated, roughly speaking, to the size of the fluctuations in the original series. The value h at $q = 2$ is equal to the well-known Hurst exponent in the case of stationary series. If the local exponent remains constant then we are observing a mono-fractal; that is, all the scales have the same (statistical) self-similarity law. By studying the order 2, we are assuming the existence of a self-similar non-Kolmogorov turbulence: one that can be modelled after the usual NOK spectra. Therefore, we will use *detrended fluctuation analysis* (DFA) to estimate the Hurst exponent of wandering time series, at different turbulence conditions. This is a good way to reveal the existence of non-Kolmogorov turbulence and its relation with the turbulence strength under different dynamical conditions.

2. THE EXPERIMENTS

We have prepared two experiments to contrast fully-developed inertial versus convective turbulence. To do so, both experiments share the same optical setup: a collimated laser beam propagating through artificial turbulence, with its wandering detected by a position detector. The emitter platform consists of a 35mW laser

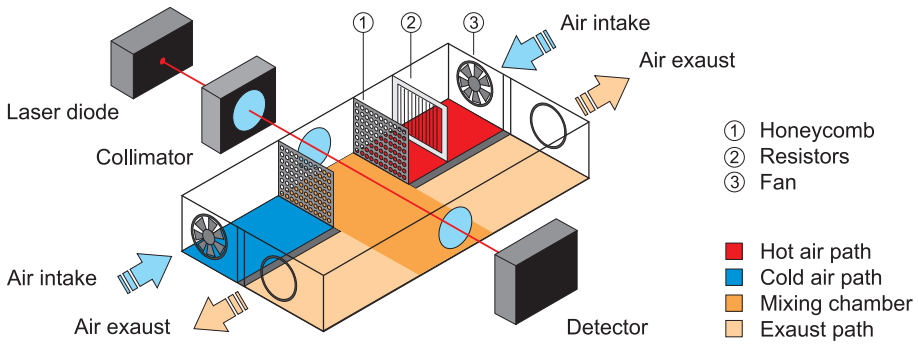

Figure 1. Experimental setup for fully-developed inertial turbulence.

diode (@635nm, DL5038-021, Thorlabs TLD001 driver) and collimating optics arranged to maintain the beam waist around 3mm along the propagation path (1.29 m long), while at the receiving platform a position sensitive detector, with an area of 1cm^2 (UDT SC-10 D) measures the centroid position of the impinging laser—with relative accuracy of 2.5μm, so very small position deflections can be measured.

For the purpose of having fully-developed inertial turbulence at stable conditions we employ a device similar to the one described in,[17] the *turbulator*: two air fluxes at different temperatures collide in a chamber producing an isotropic mix between hot and cold sources, Fig. 1. The hot source is an electric heater controlled by changing the current passing through it. The beam propagates along 0.37 m of turbulence in the turbulator chamber, with an estimated inner-scale of 6mm,[18] before exiting. Furthermore, air flow velocity is fixed so the turbulence characteristics are only due to the temperature difference. In this case, we ran four different experiments with temperature differences of 37.1, 56.3, 76.9, and 96.1 °C, and references measurements with the fans on and off. Each one of these experiments lasted 7.5 min., and the optimal sampling rate was 0.5 kHz. The wandering data was collected in 45 data files of 5000 coordinate points each.

On the other hand, convective turbulence is produced by a set of four heaters (with for heat resistors each), Fig. 2. The convective turbulence is controlled by setting the current on these heaters; we employed four digital thermometers and one anemometer to monitor the state of this turbulent flux. In this case, measurements started when the turbulence reached a quasi-stationary state. Seven independent experiments were performed, and the measurements proceeded after the four temperature probes and the anemometer stabilized—around 8 minutes in each case. Also, a reference measurement was produced with the heaters off. Each measurement extended for almost 17 min., at the same sampling rate than the experiment performed with the turbulator. This resulted in 100 data files with 5000 coordinate points each. In these experiments, we observed the following average temperatures between the probes T1 and T4 was found 1.10, 2.49, 4.04, 4.56, 6.90, 9.86, 15.42 and 15.42 °C, while the Reynolds numbers obtained from the anemometer were 3394, 6288, 6658, 7808, 7750, 7580, and 6622.

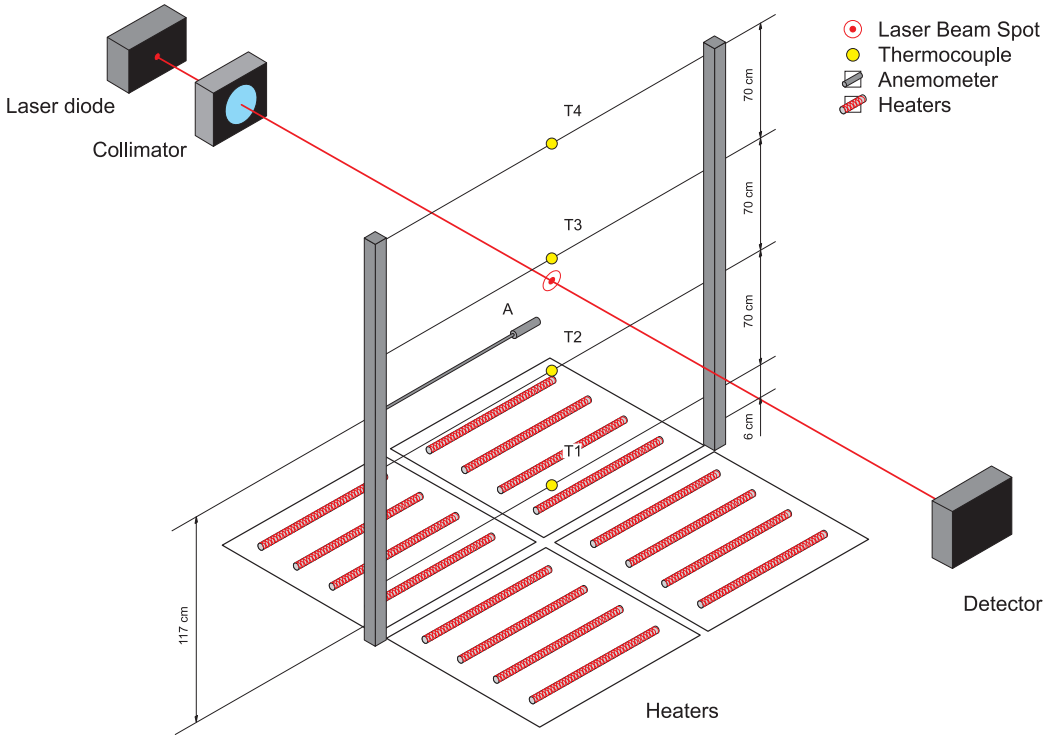

Figure 2. Experimental setup for convective turbulence.

3. ANALYSIS & CONCLUSIONS

The analysis was performed taking each archive (of 5000 data points each) as an independent realization, in both experiments—inertial and convective turbulence alike. Thus, we performed a detrended fluctuation analysis of each time series; the Hurst exponent was obtained by linear fitting a log-log plot of the scaling behaviour for the obtained order 2 fluctuation function. This fit was performed in the same scaling region for all realizations. It was determined beforehand, and chosen considering only long-correlation contributions. At the same time, the long-term beam spot size of the data series produces an associated structure constant, C_n^2, according to [19, Eq. (46), p. 189]. Observe that the Kolmogorov spectrum is tacitly assumed for C_n^2, following the now common procedure found in most of the actual literature. In the case of fully-developed inertial turbulence, we have obtained 45 coordinate pairs of structure constants and Hurst exponents, (C_n^2, H), for each axis, for the four turbulence intensities (and two more for the references) set. On the other hand, the convective turbulence provided one hundred pairs, for each axis, for the seven intensities tested.

Figure 3 shows the distribution of Hurst exponents versus structure constant produced by the turbulator. Regardless of the intensity all estimated Hurst exponents are near the Kolmogorov reference line; moreover, both Hurst exponents (horizontal and vertical) give similar values confirming the isotropy of the turbulence. As it should, since isotropy is a requirement to observe Kolmogorov turbulence. The references produce exponents near the expected values for a noise—the resolution of the position detector forbid us reducing the error on pure noise data. On average, the Hurst exponents are below the classical value 5/6. This may indicate some degree of turbulence intermittence. On the opposite side, Figure 4 is completely different. Most of the values observed are above the Kolmogorov exponent. Moreover, the exponents H are above one for the smallest values of C_n^2. We have observed this phenomenon earlier,[15] but attributed to a frail experimental setup. Clearly, there is a coupling between the structure constant and non-Kolmogorov behaviour; the Hurst exponents for each axis differ notably indicating we may be far from a fully-developed turbulence. The horizontal axis has the largest spread in power exponents and structure constants, while the vertical axis seems more well-behaved. One reason for this disagreement may reside in the lack of uniform mean flow velocity along the horizontal axis.

Although the boundary layer propagation is fairly well understood, surface-layer optical turbulence requires a more general approach. Effectively, in shear (convective) turbulence the usual procedure for evaluating C_n^2 is insufficient for qualifying its dynamical state. Due to its unpredictability and low intensity in open atmosphere, we expect similar outcomes in outdoors experiments. Moreover, the Hurst exponent consigned in this work suggest departures from the Gaussian behaviour, as $H > 1$ indicates;[20] therefore, non-Gaussian models should be pursued. Also, it should be observed that the value of the structure constant is strongly linked to the Hurst exponent asymptotic decay to 5/6, indicating a functional relationship never reported before. Future work is required to introduce corrections to the structure constant because of the deviations the Hurst exponent experiments in convective case—although, this corrections may only reduce the spread.

ACKNOWLEDGMENTS

This work was supported by Comisión Nacional de Investigación Científica y Tecnológica (CONICYT, FONDECYT Grant No. 1100753, Chile), partially by Pontificia Universidad Católica de Valparaíso (PUCV, Grant No. 123.704/2010, Chile) and Consejo Nacional de Investigaciones Científicas y Técnicas (CONICET, Argentina).

REFERENCES

1. E. Vilar and J. Haddon, "Measurement and modeling of scintillation intensity to estimate turbulence parameters in an Earth-space path," *IEEE Transactions on Antennas and Propagation* **32**, pp. 340–346, Apr. 1984.
2. B. E. Stribling, B. M. Welsh, and M. C. Roggemann, "Optical propagation in non-Kolmogorov atmospheric turbulence," in *Proc. SPIE*, J. C. Dainty, ed., pp. 181–196, June 1995.
3. R. R. Beland, "Some aspects of propagation through weak isotropic non-Kolmogorov turbulence," in *Proc. SPIE*, L. W. Austin, A. Giesen, and D. H. Leslie, eds., pp. 6–16, Apr. 1995.
4. D. Dayton, B. Pierson, B. Spielbusch, and J. Gonglewski, "Atmospheric structure function measurements with a Shack-Hartmann wave-front sensor," *Optics Letters* **17**(24), pp. 1737–17390, 1992.

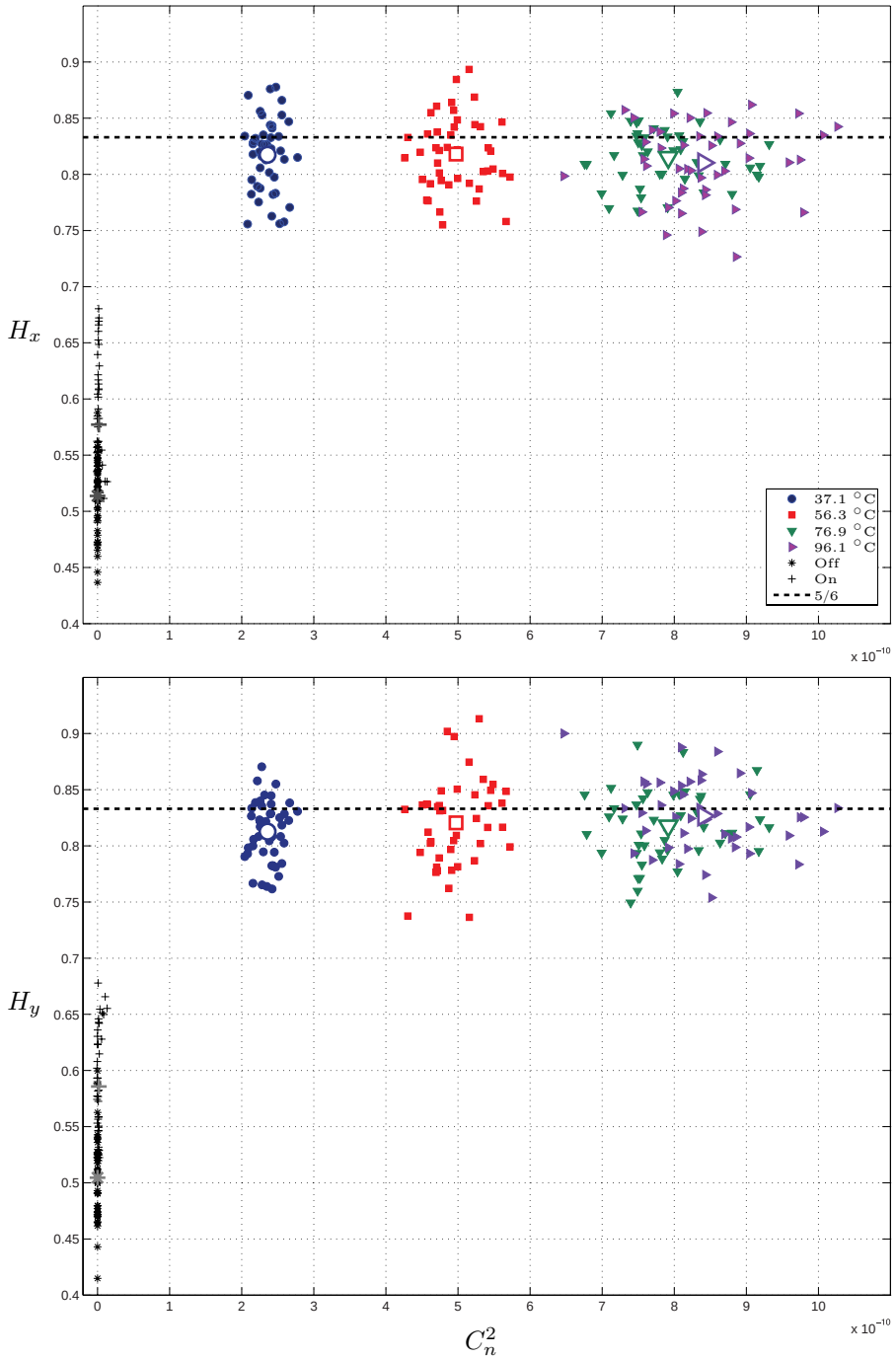

Figure 3. Hurst exponent versus structure constant for fully-developed inertial turbulence: (top) horizontal Hurst exponent, H_x, and C_n^2 pairs estimated for 45 wandering realizations; (bottom) vertical Hurst exponent, H_y, and C_n^2 pairs estimated for the same realizations. The unfilled symbols corresponds to the averages for each experiment; for the horizontal coordinate: '○' (2.36E−10 $\mathrm{m}^{-2/3}$, 0.82)@37.1°C, '□' (4.97E−10 $\mathrm{m}^{-2/3}$, 0.82)@56.3°C, '▽' (7.92E−10 $\mathrm{m}^{-2/3}$, 0.81)@76.9°C, and '▷' (8.41E−10 $\mathrm{m}^{-2/3}$, 0.81)@96.1 °C, and for the references (On, Off) the Hurst exponent is around the noise value (0.51, 0.58); for the vertical coordinate: '○' (2.36E−10 $\mathrm{m}^{-2/3}$, 0.81)@37.1°C, '□' (4.97E−10 $\mathrm{m}^{-2/3}$, 0.82)@56.3°C, '▽' (7.92E−10 $\mathrm{m}^{-2/3}$, 0.82)@76.9°C, and '▷' (8.41E−10 $\mathrm{m}^{-2/3}$, 0.83)@96.1 °C, and the noise values are 0.50 and 0.59 for On and Off, respectively.

5. T. W. Nicholls, G. D. Boreman, and J. C. Dainty, "Use of a Shack-Hartmann wave-front sensor to measure deviations from a Kolmogorov phase spectrum," *Optics Letters* **20**(24), pp. 2460–2462, 1995.
6. A. S. Gurvich and M. S. Belen'kii, "Influence of stratospheric turbulence on infrared imaging," *Journal of the Optical Society of America A* **12**, p. 2517, Nov. 1995.
7. E. Golbraikh and N. S. Kopeika, "Behavior of structure function of refraction coefficients in different turbulent field," *Appl. Opt.* **43**, pp. 6151–6156, Nov. 2004.
8. I. Toselli, L. C. Andrews, R. L. Phillips, and V. Ferrero, "Free-space optical system performance for laser beam propagation through non-Kolmogorov turbulence," *Opt. Eng.* **47**, p. 26003, Feb. 2008.
9. W. Du, S. Yu, L. Tan, J. Maa, Y. Jiang, and W. Xie, "Angle-of-arrival fluctuations for wave propagation through non-Kolmogorov turbulence," *Opt. Comm.* **282**, pp. 705–708, 2009.
10. A. Zilberman, E. Golbraikh, and N. S. Kopeika, "Some limitations on optical communication reliability through Kolmogorov and non-Kolmogorov turbulence," *Optics Communications* **283**, pp. 1229–1235, 2010.
11. X. Chu, C. Qiao, and X. Feng, "The effect of non-Kolmogorov turbulence on the propagation of cosh-Gaussian beam," *Optics Communications* **283**, pp. 3398–3403, Sept. 2010.
12. G. Wu, H. Guo, S. Yu, and B. Luo, "Spreading and direction of Gaussian-Schell model beam through a non-Kolmogorov turbulence.," *Optics letters* **35**, pp. 715–7, Mar. 2010.
13. I. Toselli, B. Agrawal, and S. Restaino, "Light propagation through anisotropic turbulence," *Journal of the Optical Society of America A* **28**, p. 483, Mar. 2011.
14. D. G. Pérez and L. Zunino, "Generalized wave-front phase for non-Kolmogorov turbulence," *Optics Letters* **33**, pp. 572–574, Mar. 2008.
15. D. G. Pérez, L. Zunino, D. Gulich, G. Funes, and M. Garavaglia, "Turbulence characterization by studying laser beam wandering in a differential tracking motion setup," *Proc. SPIE* **7476**, p. 74760D, 2009.
16. J. W. Kantelhardt, S. A. Zschiegner, E. Koscielny-Bunde, A. Bunde, S. Havlin, and H. E. Stanley, "Multifractal Detrended Fluctuation Analysis of Nonstationary Time Series," *Physica A* **316**, pp. 87–114, 2002.
17. O. Keskin, L. Jolissaint, and C. Bradley, "Hot-air optical turbulence generator for the testing of adaptive optics systems: principles and characterization," *Appl. Opt.* **45**, pp. 4888–4897, July 2006.
18. D. G. Pérez, A. Férnandez, G. Funes, D. Gulich, and L. Zunino, "Retrieving atmospheric turbulence features from differential laser tracking motion data," pp. 853508–853508–11, Nov. 2012.
19. L. C. Andrews and R. L. Phillips, *Laser Beam Propagation through Random Media*, SPIE, 1998.
20. G. Samorodnitsky and M. S. Taqqu, *Stable Non-Gaussian Random Processes: Stochastic Models with Infinite Variance*, Stochastic modeling, Chapman & Hall/CRC, New York, 1994.

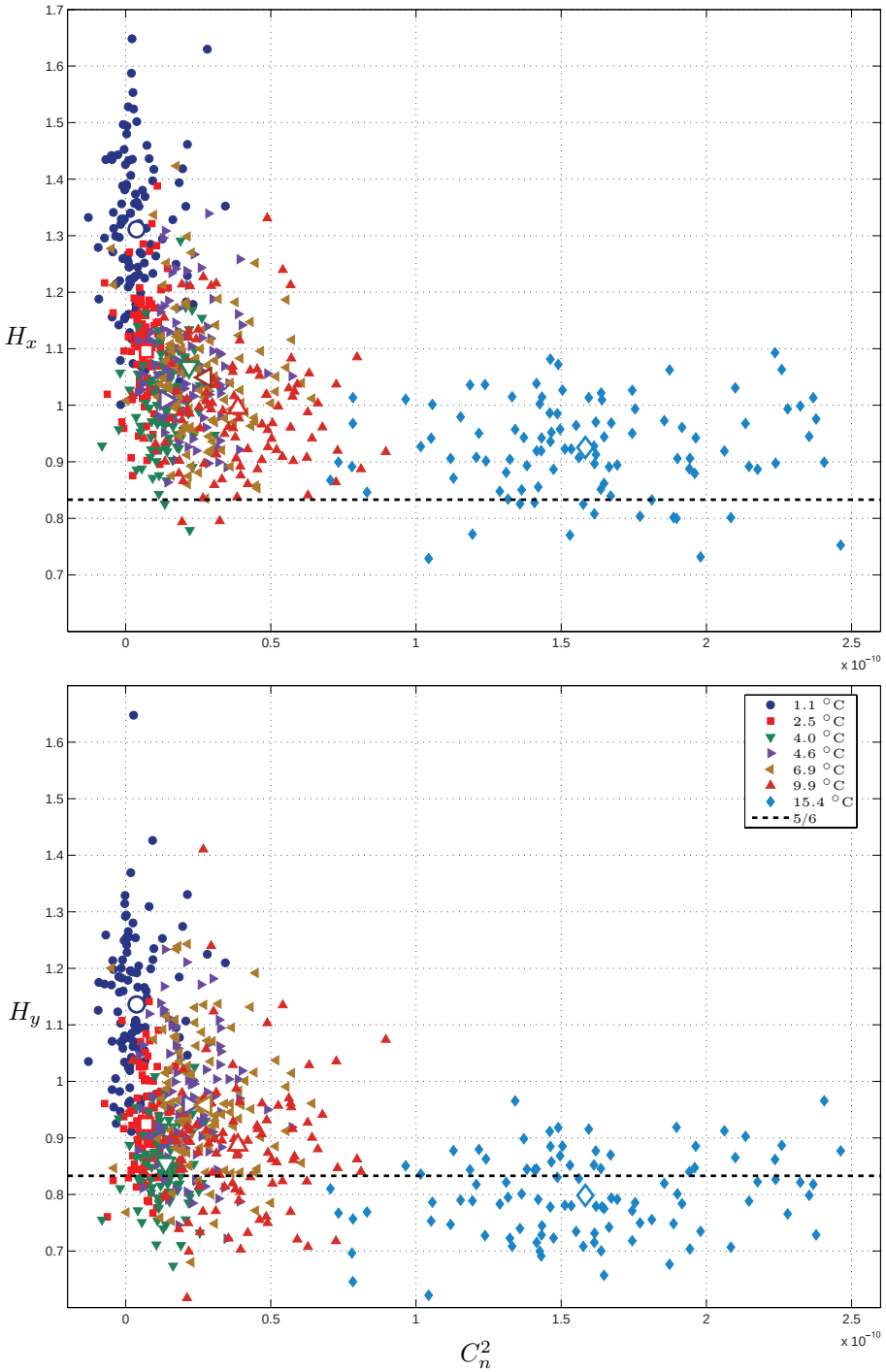

Figure 4. Hurst exponent versus structure constant for convective turbulence: (top) horizontal Hurst exponent, H_x, and C_n^2 pairs estimated for 100 wandering realizations; (bottom) vertical Hurst exponent, H_y, and C_n^2 pairs estimated for the same realizations. The unfilled symbols corresponds to the averages for each experiment; for the horizontal coordinate: '○' (3.77E−12 $\mathrm{m}^{-2/3}, 1.09$)@1.1°C, '▫' (7.15E−12 $\mathrm{m}^{-2/3}, 1.01$)@2.5°C, '▽' (1.37E−11 $\mathrm{m}^{-2/3}, 1.01$)@4.4°C, '▷' (2.18E−11 $\mathrm{m}^{-2/3}, 1.07$)@4.6°C,'◁' (2.76E−11 $\mathrm{m}^{-2/3}, 1.05$)@6.9°C,'△' (3.86E−11 $\mathrm{m}^{-2/3}, 0.99$)@9.9°C, and '◇' (1.58E−10 $\mathrm{m}^{-2/3}, 0.92$)@15.4°C; for the vertical coordinate: '○' (3.77E−12 $\mathrm{m}^{-2/3}, 1.14$)@1.1°C, '▫' (7.15E−12 $\mathrm{m}^{-2/3}, 0.92$)@2.5°C, '▽' (1.37E−11 $\mathrm{m}^{-2/3}, 0.85$)@4.4°C, '▷' (2.18E−11 $\mathrm{m}^{-2/3}, 0.96$)@4.6°C,'◁' (2.76E−11 $\mathrm{m}^{-2/3}, 0.96$)@6.9°C,'△' (3.86E−11 $\mathrm{m}^{-2/3}, 0.89$)@9.9°C, and '◇' (1.58E−10 $\mathrm{m}^{-2/3}, 0.80$)@15.4°C. References correspond to the observed exponents in the inertial turbulence case.